Structure and Shape Effects of Molecular Glue on Supramolecular Tubulin Assemblies

Matteo Garzoni,[†] Kou Okuro,[‡] Noriyuki Ishii,[§] Takuzo Aida,[‡] and Giovanni M. Pavan*[,†]

[†]Department of Innovative Technologies, University of Applied Science of Southern Switzerland, Galleria 2, Manno 6928, Switzerland, [‡]Department of Chemistry and Biotechnology, School of Engineering, The University of Tokyo, 7-3-1 Hongo, Bunkyo-ku, Tokyo 113-8656, Japan, and [§]Biomedical Research Institute, National Institute of Advanced Industrial Science and Technology (AIST), Central-6, 1-1-1 Higashi, Tsukuba-shi, Ibaraki 305-8566, Japan

ABSTRACT

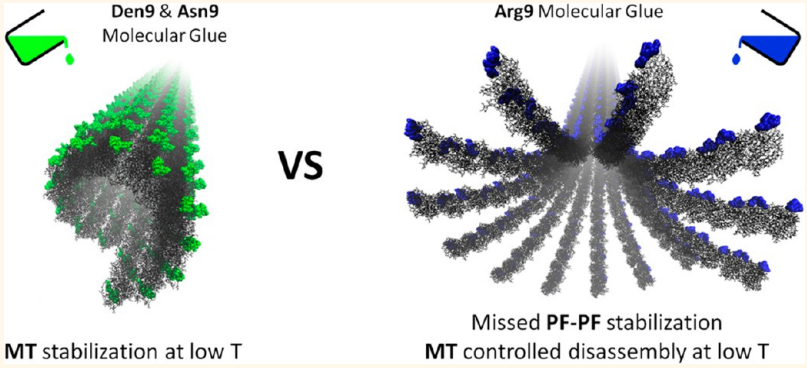

The possibility to arrange biological molecules into ordered nanostructures is an important issue in nano- and biotechnology. Nature offers a wide range of molecular "bricks" (*e.g.*, proteins, oligonucleotides, *etc.*) that spontaneously assemble into more complex hierarchical systems with unique functionalities. Such molecular building blocks can be also used for the construction of nanomaterials with peculiar properties (*e.g.*, DNA origami). In some cases, molecular glues able to bind biomolecules and to induce their assembly can be used to control the final structure and properties in a convenient way. Here we provide molecular-level description of how molecular glues designed to stick to the surface of microtubules (MTs) can control and transform the α/β-tubulin assembly upon temperature decreasing. By means of all-atom molecular dynamics (MD) simulations, we compared the adhesion to the MT surface of three molecular glues bearing the same guanidinium ion surface adhesive groups, but having different architecture, *i.e.*, linear or dendritic backbone. Our evidence demonstrates that the adhesive properties of the different molecular glues are dependent on the shape they assume in solution. In particular, adhesion data from our MD simulations explain how globular- or linear-like molecular glues respectively stabilize MTs or transform them into a well-defined array of α/β-tubulin rings at 15 °C, where MTs naturally depolymerize. The comprehension of the MT transformation mechanism provides a useful rationale for designing *ad hoc* molecular glues to obtain ordered protein nanostructures from different biological materials.

KEYWORDS: molecular glue · microtubule · protein nanostructure · tubulin assembly · tubulin rings · protein origami · dendrimer

Biological systems employ self-assembly for constructing materials with high structural and functional complexity.[1,2] Examples of such materials include nucleic acids (DNA and RNA), which are composed of polynucleotide strands. According to the base sequence, the strands self-assemble into higher-order structures such as double-stranded helices, hairpin loops, and so forth through hydrogen bonding interactions between specific base pairs. Recently, the extreme selectivity of the DNA hybridization has been successfully exploited to construct elaborate 2D[3,4] or 3D[5−7] nanoarchitectures called "DNA origami".

Proteins also assemble generating a variety of unique structures including tubes,[8] fibers,[9] two-dimensional layers,[10] and hollow spheres[11,12] by electrostatic, hydrogen bonding, and van der Waals interactions. Since proteins bear various functional groups, namely, the side chains of amino acids, and are easily functionalized by chemical modification, they are attractive platforms for

* Address correspondence to giovanni.pavan@supsi.ch.

Received for review October 30, 2013 and accepted December 18, 2013.

Published online December 18, 2013
10.1021/nn405653k

constructing functional nanomaterials. In order to realize desired nanostructures made of proteins (*i.e.*, "protein origami"), engineered proteins expressing artificial binding motifs have been developed.[13−15] Another strategy is to utilize "molecular glues"[16,17] able to bind proteins[18] and to induce their assembly.[19,20]

Microtubules (MTs) are tubular assemblies of α/β-tubulin protein heterodimers. They are generated by the cylindrical side-to-side coupling of single protofilaments (PFs) that are, in turn, formed by the linear head-to-tail assembly of α/β-tubulins.[8] Typically, MTs have lengths ranging from 200 nm to 25 μm and diameters of ~25 nm. MT polymerization and depolymerization are delicate processes sensitive to the external conditions; MT depolymerization starts spontaneously for temperatures lower than the physiological one.[21]

Recently, we have looked at the possibility to control MTs by using synthetic scaffolds functionalized with sticky surface groups as molecular glues. In particular, we verified that after treatment at 37 °C with a dendritic molecular glue (**Den9**, Figure 1a) bearing nine guanidinium ion (Gu^+) pendants at its periphery, the entire structure of MTs is fully stabilized also at the lower temperature of 15 °C, where MTs spontaneously depolymerize into α/β-tubulin heterodimers (Figure 1b).[22] Interestingly, if the dendritic **Den9** is substituted with a linear polymeric molecular glue, *i.e.*, **Arg9** (Figure 1c), an arginine nonamer with the same surface functionalization of **Den9** but having a different scaffold architecture, MTs are transformed into a well-defined and stable array of rings (Figure 1d,f) when temperature is decreased from 37 to 15 °C.[23]

Even if the mechanism of adhesion of **Den9** and **Arg9** to the MT surface is based on the same kind of interaction, salt-bridges between Gu^+ ions and protein COO^- groups, and the two molecular glues differ only in the backbone structure, they give rise to completely different tubulin-based supramolecular structures upon temperature decreasing, which initially suggested the existence of a direct link between molecular glue functionality and scaffold architecture.

However, we found that full MT stabilization at low temperature is achieved also by using a third molecular glue, **Asn9**, a linear polymer bearing nine Gu^+-terminated triethylene glycol (TEG) spacers as side chains (Figure 1f),[22] which offered a more complicated and unclear scenario.

Understanding how different molecular glues stick to the MT surface is a key issue to rationalize the mechanisms of MT stabilization and of MT transformation into a different α/β-tubulin nanosctructure at low temperature. In fact, it would constitute an important step for learning how to control molecular glue behavior, and thus toward the rational design of dedicated molecular glues for realizing arbitrary α/β-tubulin "protein origami".

In this work, we have used all-atom molecular dynamics (MD) simulations to study the adhesion of the three molecular glues (**Arg9**, **Den9**, and **Asn9**) onto the MT surface, aiming at elucidating the origin and the mechanism of formation of different tubulin-based nanostructures.

RESULTS AND DISCUSSION

The computational strategy adopted for this complex study is based on the simulation approach reported recently by our group for investigating the adhesion of positively charged dendrons on the negatively charged protein surface of capsid viruses.[20] Our approach is essentially divided in two steps. First, it was necessary to understand how molecular glues "appear" in the real environment. In fact, once molecules are immerged in solution, they can assume a conformation looking totally different from the extended chemical structures reported in Figure 1, which can have a dramatic effect on the final properties. After we gained information about the conformation assumed by **Arg9**, **Den9**, and **Asn9** in the real environment, we aimed at studying the adhesion of the different molecular glues to the MT surface.

Thus, we first created molecular models for **Arg9**, **Den9**, and **Asn9** molecular glues according to the same procedure followed by our group for similar previous studies.[24,25] At neutral pH, all surface Gu^+ groups were assumed as charged, and all molecular glues bear a total positive charge of +9e. These molecular models were immerged in a simulation box containing explicit solvent molecules and then equilibrated at 37 °C and 1 atm of pressure through a first series of MD simulations in order to understand the shape and conformation assumed by **Arg9**, **Den9**, and **Asn9** in solution (computational details are available in the Computational Methods section, and in the Supporting Information (SI)).

MD simulations evidenced that the three molecular glues have a different behavior in solution. Particularly, while the branched **Den9** folds into a globular structure, **Arg9** maintains its linear character. Conversely, during the MD run, **Asn9** loses completely its linearity assuming a globular shape similar to that of **Den9**. These observations are supported by the size data (*i.e.*, the radius of gyration, R_g) extracted from the MD simulations of the three molecular glues in solution (see SI for details). The initial open unfolded configurations of **Den9** and **Asn9** (R_g of 16 and 14.2 Å, respectively) collapse early during the MD runs. At the equilibrium, **Den9** and **Asn9** have the same size, being their R_g equal to 9.0 ± 0.4 and 9.0 ± 0.3 Å, respectively. On the other hand, the size of **Arg9** (R_g = 8.3 ± 0.8 Å) does not change substantially during the MD simulation, and this molecular glue maintains its linear shape. The PEG spacers of **Den9** and **Asn9** are structurally more flexible than the alkyl spacers of **Arg9**, and this allows **Den9** and **Asn9** to fold assuming a globular shape in solution, consistent with the strong folding

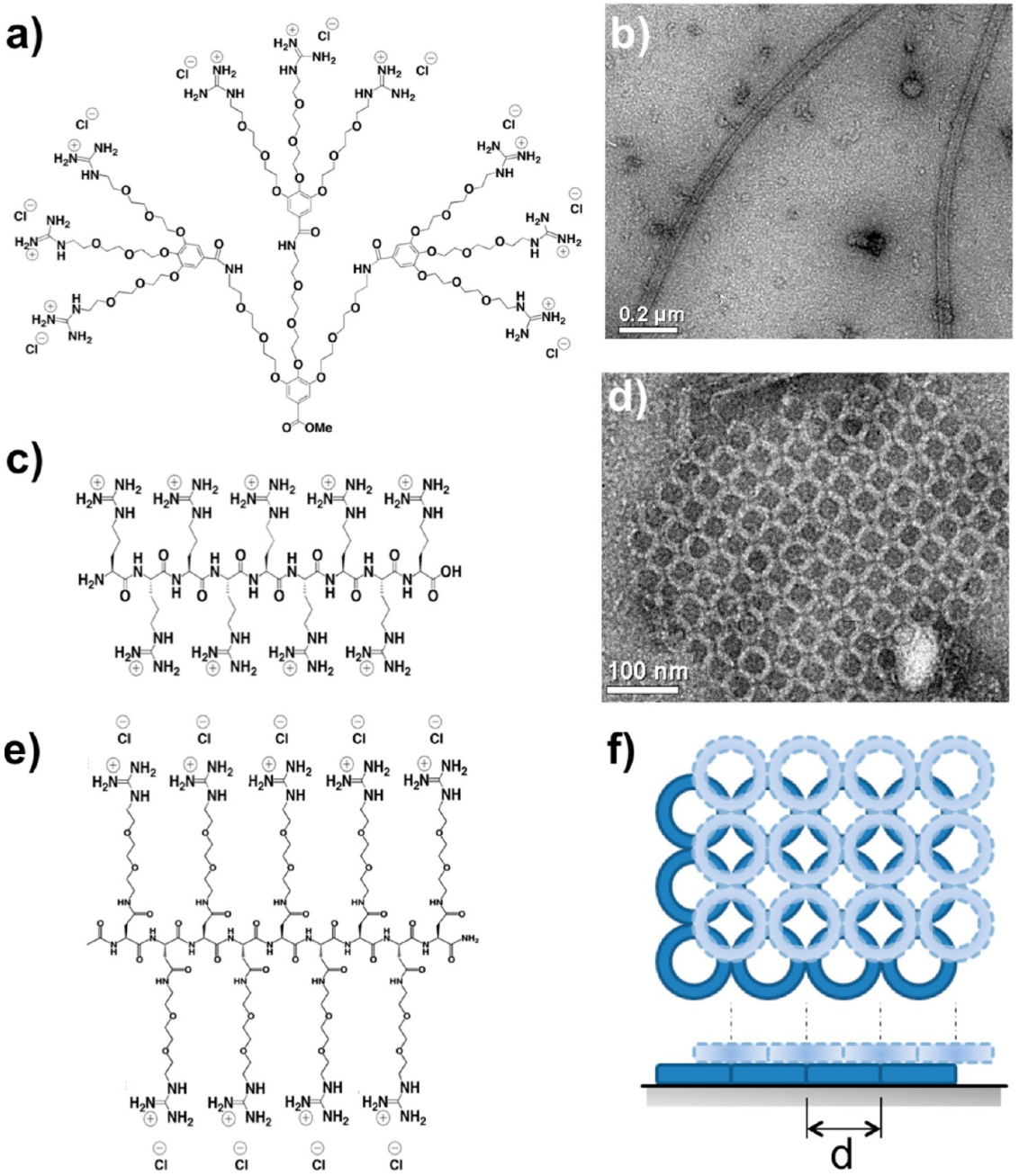

Figure 1. Different molecular glues stabilize different tubulin supramolecular structures at low temperature. When the temperature is decreased to 15 °C, the dendritic Den9 (a) molecular glue stabilizes the entire MT structure (b). On the other hand, the linear Arg9 (c) molecular glue transforms MTs into a well-defined array of tubulin rings at low temperature (d). (e) Unlike Arg9, another linear molecular glue, Asn9, stabilizes the whole MT structure at 15 °C, acting like the dendritic Den9. (f) The tubulin rings generated by Arg9 are arranged according to a well-defined alternated square crystal packing with a measured axial distance between the rings of $d = 49.0 \pm 1.0$ nm.[23]

typical of polyethylene glycol (PEG), which constitutes large part of their scaffold, in water.[25] Conversely, **Arg9** does not have the same option and does not collapse in water.

Thus, despite the different backbone architecture (linear *versus* branched scaffold), in solution **Asn9** is more similar to the dendritic **Den9** than to the linear **Arg9**, both in terms of size and shape. This point is particularly important because, as said, the conformation assumed by molecular glues in the real environment is of key importance for their adhesion to the MT surface. Figure 2a shows equilibrated snapshots taken from the MD simulations of the three molecular glues.

The second part of our work pertains to the study of molecular glues adhesion to the MT surface. A molecular model of a 13 PFs MT (Figure 2b) was first obtained as previously reported in literature (see Computational Methods section).[26−28] Even if MTs naturally depolymerize at 15 °C, their structures can be fully stabilized also at low temperature (15 °C) when they are treated

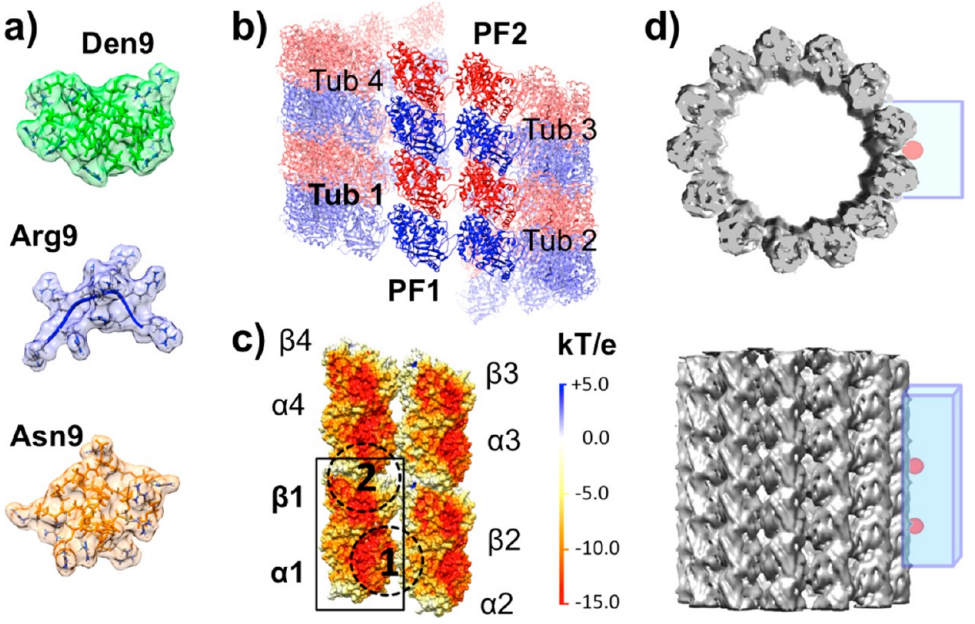

Figure 2. Molecular models. (a) Equilibrated (final) MD snapshots of the Den9, Arg9, and Asn9 molecular glues. (b) A portion of MT was selected as composed of 4 α/β-tubulin dimers (Tub 1 to 4) coupled both axially (intra-PF) and laterally (inter-PF). (c) The electrostatic potential was calculated on the MT surface. Red regions identify higher negative charge density, which constitute potential binding sites for the positively charged molecular glues. Two binding sites were identified (1 and 2), between α1 and α2 and between β1 and α4 tubulins, respectively, where the binding of molecular glue can stabilize the tubulin dimers both along and between PFs. (d) A periodic box was constructed around the selected MT region, containing two equilibrated Den9, Arg9, or Asn9 molecules and filled with explicit solvent molecules.

with **Den9** and **Asn9** molecular glues.[22] Thus, in principle, molecular glue is assumed to be capable of inducing both intra-PF and inter-PFs reinforcement in the MT structure. For this reason, a portion of MT was selected for the MD simulations composed of four α/β-tubulin dimers belonging to two laterally bound PFs (**PF1** and **PF2**, Figure 2b). Such system allows for the study of the molecular glue adhesion both along a single PF and between different PFs, and it is well suited for the study of the molecular interactions with the MT surface.[29,30]

All three molecular glues bear nine surface guanidinium ion (Gu^+) pendants that can stick to α/β-tubulin amino acids *via* salt-bridges. The adhesion of molecular glue to the MT surface is thus controlled by a combination of electrostatic and H-bonding interactions. In order to gain more information about the MT surface, according to the strategy previously adopted for similar studies on the electrostatic adhesion of charged dendrons to the oppositely charged protein surface of CCMV virus capsids,[20] we calculated the electrostatic potential in the MT selected region (Figure 2c) as described in detail in the Computational Methods section.[31]

Red areas in Figure 2c represent high negative surface charge, and potential binding sites for the positively charged molecular glues along the MT surface. Conceptually, once glue molecules are introduced in the real system, they are strongly attracted by the red regions present on the MT surface due to electrostatic effect. Thus, the probability to have molecular glue adhesion in proximity these zones is very high. Even if high negative charge is present on the entire MT surface, the interface regions between different α/β-tubulin dimers are the most important ones for MT stabilization, and thus for our study. In fact, a glue molecule binding just to a single tubulin would not reinforce the tubulin−tubulin assembly when the temperature decreases.

Considering **Tub 1** as the reference protein in the system, two binding sites (**1** and **2**) were identified between tubulins **α1** and **α2**, and between **β1** and **α4** respectively, where the binding of molecular glue might reinforce the tubulin−tubulin coupling along the same PF and the adhesion between different PFs (Figure 2c). Binding sites **1** and **2** are representative of those "weak" regions present all along the α/β-tubulin assembly that are critical for MT stabilization or depolymerization, and that can be reinforced thanks to molecular glue adhesion. It is worth noting that tubulin−tubulin binding sites **1** and **2** are morphologically very different. In fact, while the PF surface is flat and uniform, the PF−PF interface (lateral α/β-tubulin coupling) appears as a long groove (Figure 2d).

Two equilibrated **Arg9**, **Den9**, and **Asn9** molecules were then placed in correspondence of the **1** and **2** binding sites and in close proximity of the MT surface.[20] This 2:1 stoichiometry between molecular glue and **Tub 1** was consistent with the experiments.[23] The molecular models used for the simulations consist of

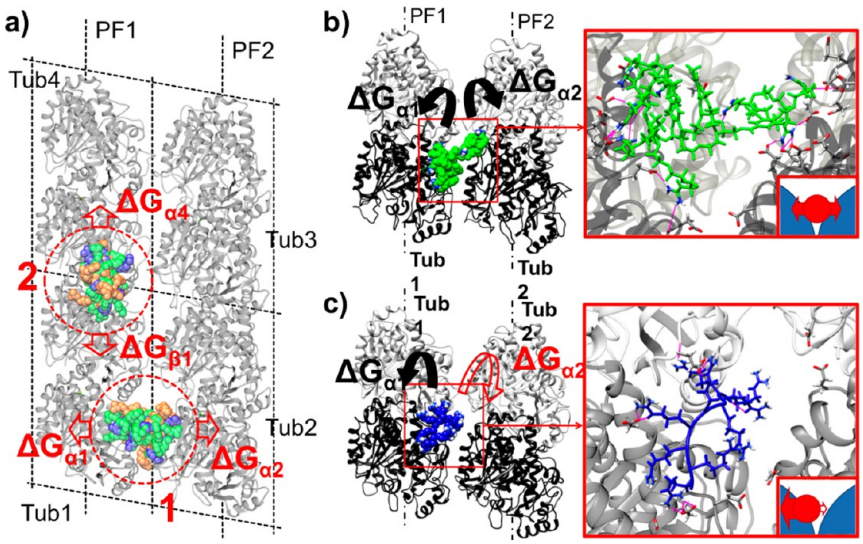

Figure 3. Gluing action by molecular glue. (a) Starting configurations of the simulated systems. Each molecular system is composed of four α/β-tubulin dimers (Tub 1 to Tub 4, gray ribbons) and two molecules of each molecular glue initially placed in correspondence of the 1 and 2 binding sites and in close proximity of the MT surface. Den9, Arg9, and Asn9 are colored in green, blue, and orange, respectively. Water molecules and counterions are not shown for clarity. (b,c) Equilibrated (last) snapshots taken from the MD simulations at 15 °C: detail of the Den9 (b) and Arg9 (c) glue binding behavior in binding site 1. The intra-PF and inter-PFs reinforcements induced by the molecular glue were interpreted as the interaction-free energies of binding (ΔG_{nn}) between each glue molecule and the involved tubulin protein. $\Delta G_{\beta 1}$ and $\Delta G_{\alpha 4}$ in position 2 quantify the adhesion of the glue to proteins belonging to the same PF. $\Delta G_{\alpha 1}$ and $\Delta G_{\alpha 2}$ at the PF−PF interface are indicative of the inter-PF stabilization induced by the glue. The globular shape of Den9 allows for strong interactions with both PFs (Tub 1 and Tub 2) in position 1 (H-bonds are represented in pink). (c) On the other hand, in the same position Arg9 binds successfully only to Tub1 but not to Tub2 (a total of eight different starting configurations were studied for Arg9 in binding site 1).

a periodic box containing four tubulin proteins and two glue molecules, and filled with explicit solvent molecules (details in the Computational Methods section). A total of three molecular systems were thus simulated: **MT**+**Den9**, **MT**+**Arg9**, and **MT**+**Asn9**.

At this stage, we aimed at gaining information through MD simulations about molecular glues adhesion to the MT surface in proximity of binding sites **1** and **2**, which, as said, represent critical points along the MT structure for MT reinforcement or depolymerization. All systems were equilibrated for 100 ns through a first series of NPT MD simulation at 37 °C and 1 atm of pressure. During the MD runs, all molecular glues showed strong adhesion to the MT surface. Temperature was then decreased to 15 °C, and each system underwent additional 100 ns of NPT MD simulation. Detailed description of all simulated systems and of the simulation protocol is reported in the Computational Methods section and in the SI.

The adhesion of molecular glues to the MT surface was estimated directly from the MD simulations at both 37 and 15 °C as the free energy of binding (ΔG) between the glue molecules and the MT surface. In general, the more negative the ΔG value, the stronger the adhesion of the molecular glue to the MT surface (full ΔG data are reported in the SI).

Moreover, since the MT stabilization at 15 °C is associated to the α/β-tubulin dimer−dimer assembly reinforcement induced by molecular glue, the latter was evaluated *via* simple decomposition of ΔG as the energetic adhesion of each glue molecule to the single proteins of interest in the system (ΔG_{nn} in Figure 3), *i.e.*, **Tub1** and **Tub4** for single PFs reinforcement, and **Tub1** and **Tub2** for what pertains to PF−PF assembly stabilization. Details about the energetic analysis procedure are available in the Computational Methods section and in the SI.

As aforementioned, for the sake of molecular glue-induced tubulin−tubulin coupling reinforcement, it is necessary that at low temperature each glue molecule can bind successfully more than one tubulin protein at a time.

Data from MD simulations show that all molecular glues can stabilize single PFs at 15 °C, interacting productively with both **Tub1** and **Tub4** ($\Delta G_{\beta 1}$ and $\Delta G_{\alpha 4}$ in Table 1). On the other hand, the glues behavior at the PF−PF interface (binding site **1**) is very different. Table 1 collects the ΔG_{nn} values extracted from the MD simulations related to the molecular glue-induced tubulin−tubulin assembly stabilization at the critical temperature of 15 °C. In fact, the globular shape of **Den9** fits perfectly with the **PF1**−**PF2** interface groove, allowing for strong interactions with both PFs at low temperature ($\Delta G_{\alpha 1}$ and $\Delta G_{\alpha 2}$ of -35.2 ± 3.6 and -28.1 ± 3.0 kcal mol^{-1} respectively). Despite its native structural linearity, and thanks to the folded globular shape assumed in solution, also **Asn9** molecular glue allows for inter-PF coupling reinforcement ($\Delta G_{\alpha 1} = -43.2 \pm 4.1$ kcal mol^{-1} and $\Delta G_{\alpha 2} = -29.7 \pm 3.1$ kcal mol^{-1}). Consistent with the compact globular shape assumed

TABLE 1. Molecular Glue-Induced Tubulin−Tubulin Assembly Stabilization at 15 °C[a]

ΔG_{nn}[b]	$\Delta G_{\beta 1}$[c]	$\Delta G_{\alpha 4}$[c]	$\Delta G_{\alpha 1}$[d]	$\Delta G_{\alpha 2}$[d]
Den9+MT	−22.9 ± 2.4	−20.3 ± 2.3	−35.2 ± 3.6	−28.1 ± 3.0
Arg9+MT[e]	−24.3 ± 2.9	−19.6 ± 2.0	−34.1 ± 4.3[e]	−1.9 ± 0.3[e]
Asn9+MT	−21.9 ± 2.1	−19.1 ± 2.0	−43.2 ± 4.1	−29.7 ± 3.1

[a] ΔG_{nn} data are expressed in kcal mol^{-1} and are related to those single α and β tubulins in the MT wall involved in the binding with molecular glue. [b] Molecular glue-induced stabilization (ΔG_{nn}) energy values are calculated from the equilibrated phase (the last 50 ns) of MD simulations at 15 °C. [c] $\Delta G_{\beta 1}$ and $\Delta G_{\alpha 4}$ values are related to the glue adhesion in binding site **2** and are representative of the stabilization of single PFs induced by molecular glue. [d] $\Delta G_{\alpha 1}$ and $\Delta G_{\alpha 2}$ values are related to the glue adhesion in binding site **1** and are thus representative of the PF−PF assembly stabilization induced by molecular glue. [e] The reported $\Delta G_{\alpha 1}$ and $\Delta G_{\alpha 2}$ values for the **MT**+**Arg9** case are averaged over a total of eight MD simulations relative to different **Arg9** starting configurations.

by **Den9** and **Asn9** in solution, where Gu^+ adhesive groups are present all over the molecular glue surface, these data are well representative, in general, of the adhesion of **Den9** and **Asn9** molecular glues in the PF−PF interface cavities, and prove that indeed **Den9** and **Asn9** molecular glues can stick to multiple tubulin proteins from different PFs along the MT wall. In this way, **Den9** and **Asn9** molecular glue allow also for PF−PF assembly reinforcement, stabilizing the whole MT structure as it is verified experimentally.[22]

On the contrary, MD simulation of the **MT**+**Arg9** system showed that the spacing between the positively charged groups of **Arg9** is so reduced that as soon as a first productive interaction occurs between the glue and one tubulin, this molecular glue collapses over that protein, so that the interaction with a second tubulin target belonging to a different PF is compromised.

Because of the linear shape of **Arg9** molecular glue, and in order to exclude possible system-dependency issues, this observation was challenged by exploring seven other possible configurations/orientations of **Arg9** in proximity of binding site **1** and by running as many independent additional MD simulations (see Computational Methods section and the SI for details).

The same result for a total of eight different starting configurations of **Arg9** in position **1** proves that indeed this molecular glue is not capable of reinforcing the PF−PF adhesion. Average energy data extracted from all eight MD simulations pertaining to this case demonstrate that, after productive binding occurs with a first tubulin ($\Delta G_{\alpha 1}$ = −34.1 ± 4.3 kcal mol^{-1} on average), the adhesion with a second one belonging to a different PF is unflavored by more than 1 order of magnitude ($\Delta G_{\alpha 2}$ reduced to −1.9 ± 0.3 kcal mol^{-1} on average). In fact, our simulations show that **Arg9** molecular glue must undergo considerable stretching in order to bind both proteins from different PFs (see SI, Figure S6).

In summary, these results indicate that the adhesion of different molecular glues to the MT surface is controlled by the shape assumed by molecular glues in the real environment rather than by their chemical structure (linear or branched backbone). In fact, the adhesion of **Asn9** to MT is similar to that of **Den9** (Figure 4) and different from that of **Arg9**, consistent with what was said in precedence about the shape assumed by these molecules in solution. Our evidence suggests that while **Den9** and **Asn9** can stabilize the entire MT structure at 15 °C, **Arg9** allows just for reinforcement of single PFs, but it fails in stabilizing PF−PF pairing. Indeed in this case molecular shape, recently highlighted by Tomalia as one critical parameter to understand interactions at the nanoscale,[32,33] plays a fundamental role in controlling molecular glue adhesion to MTs.

The molecular picture provided by the MD simulations also suggests that the stable tubulin rings generated by **Arg9** at 15 °C apparently originate from the missed PF−PF reinforcement by **Arg9**, and from the following MT depolymerization into single PFs. This hypothesis was challenged by the creation of an additional molecular model, aiming at representing one of the unbound **Arg9**-stabilized PFs originating from MT depolymerization at 15 °C (Figure 5a). **PF2** was thus deleted from the previously simulated systems, and only **Tub1** and **Tub4**, belonging to **PF1**, were considered. An additional **Arg9** molecule (**Arg9$_3$**) was added along the PF for symmetry (Figure 5b). The resulting **Arg9**-bound PF was immerged into a periodic water box extending 15 Å in all directions from the solute atoms, allowing for eventual PF deformations (see SI). This additional system (**PF**+**Arg9**) was equilibrated for 200 ns of NPT MD simulation at 15 °C and 1 atm of pressure.

At the equilibrium, the **Arg9**-reinforced PF bends by an angle of $\varphi = 19° \pm 1.1°$ between **Tub1** and **Tub4** dimers (Figure 5b).

Considering an α/β-tubulin dimer length of 8.3 ± 0.6 nm, the bent tubulin dimer−dimer complex (Figure 5b,c) replicated in space gives rise to a tubulin ring with diameter of ∼50.1 nm (Figure 5c), corresponding to ∼18−19 tubulins per ring, that is consistent with the experimental measured diameter of 49.0 ± 1.0 nm (Figure 5d).[23] This result is in good agreement also with other previously reported monodispersed tubulin rings formed by GDP-bound tubulin that, however, were more heterogeneous and far from being stable in solution.[34,35] Thus, this evidence shows that the precise array of tubulin rings obtained at 15 °C[23] originates from **Arg9**-stabilized PFs that bend and convolve into "collapsed helices",[36,37] very stable at low temperature because of the stabilizing action by **Arg9** molecular glue.

The outcomes of this study suggest possible criteria for the design of molecular glues to manipulate the tubulin supramolecular structure. In fact, molecular glues functionalized with Gu^+ ions surface groups

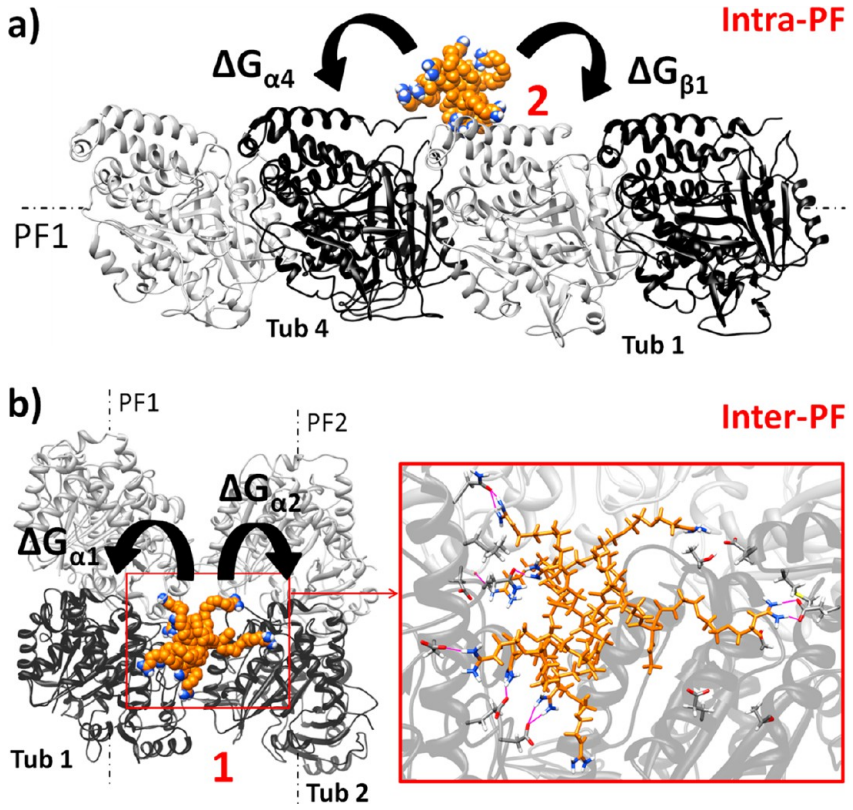

Figure 4. Full MT stabilization at 15 °C by Asn9. Asn9 molecular glue is colored in orange; explicit water molecules and neutralization ions are not shown for clarity. The folded shape of Asn9, closer to that of Den9 than to Arg9, allows for strong interactions with more than one tubulin protein both along the same PF (a) and between different PFs (b). Inset: H-bonds formed between Asn9 and Tub1 and Tub2 are colored in pink (PF−PF adhesion reinforcement).

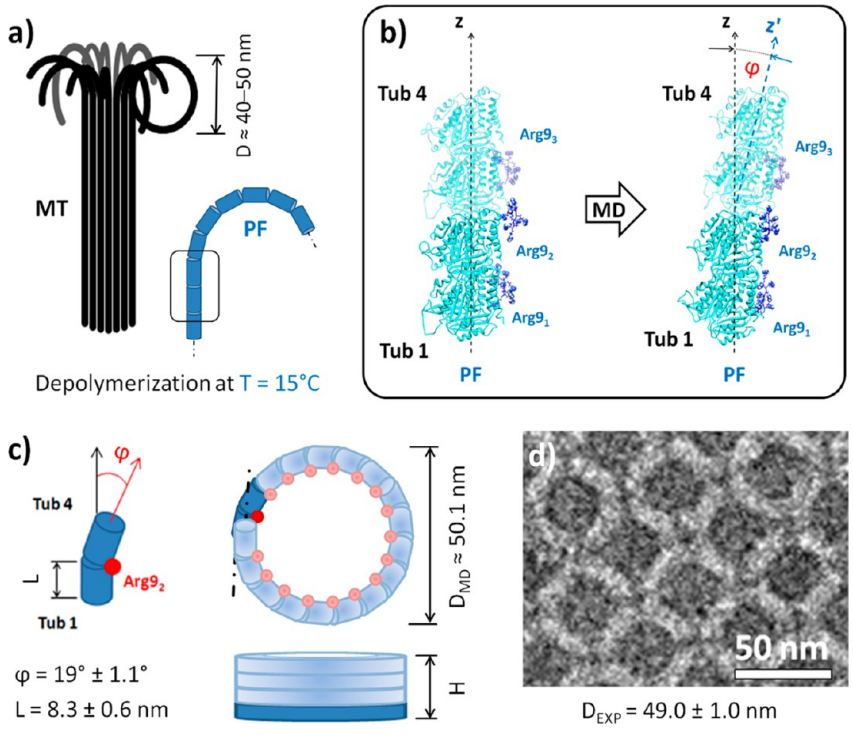

Figure 5. Origin of the tubulin ring array. (a) Scheme of Arg9-bound MT depolymerization at 15 °C. Arg9 stabilizes only single PFs but not the PF−PF adhesion. Thus, at 15 °C MTs disassemble into Arg9-bound PFs. (b) At the equilibrium, the axial assembly of Tub1 and Tub4 dimers bends of $\varphi = 19° \pm 1.1°$. (c) Considering a tubulin dimer length (L), and the bent PF portion replication, Arg9-bound PFs convolve into tubulin rings with diameter of ~50.1 nm, in optimal agreement with the tubulin ring diameter measured experimentally (d).[23]

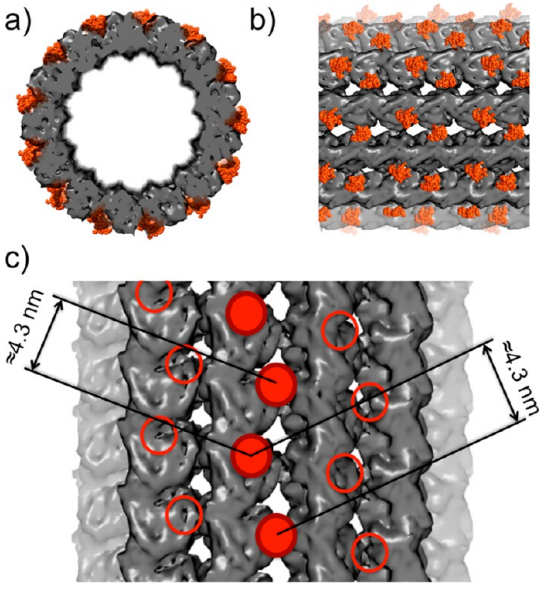

Figure 6. Binding spots at the MT surface. (a,b) Top and side view of the MT (electron microscopy EM-map) reinforced by Asn9 molecular glue (orange). (c) The binding sites for molecular glue (binding sites 1 and 2) are arranged at an average distance of ~4.3 nm from each other.

and having a globular shape and size comparable to that of **Den9** and **Asn9** (a folded R_g of ~1 nm) should allow stabilization of the entire MT structure at low temperature. On the other hand, smaller molecular glues which maintain a linear character in solution would work similarly to **Arg9**, transforming the MTs into tubulin ring arrays similar to that in Figure 1 generated by **Arg9** at 15 °C.

In general, since the distance between binding sites **1** and **2** at the MT surface is of ~4.3 nm (Figure 6), only molecular glues with a folded size (R_g) lower than ~2 nm would allow for a complete interaction with all binding sites (**1** and **2**) present at the MT surface. In fact, larger charged molecular candidates would interfere with each other, producing discontinuities in the molecular glue adhesion to the MT surface, and leading to a disordered MT disassembly upon temperature decreasing. In this perspective, the design of possible alternatives could also benefit from existing branched scaffolds, *e.g.*, small generations (G1-G3) of PAMAM dendrimers,[51] PPI dendrimers (G2-G4),[52] or more recent triazine-based examples[53] (G1-G3) could be functionalized with Gu^+ ion surface groups allowing to explore the effect of different molecular glues on MT stabilization at low temperature.

Moreover, new molecular glues capable of transforming the MT structure into a tubulin ring array at low temperature like **Arg9** could be in principle designed starting from **Den9** and **Asn9** by respectively deleting some branches (*e.g.*, changing the branching motif from a three-branched into a two-branched scaffold), or in the latter case, by shortening the PEG spacers.

CONCLUSIONS

In conclusion, we have used molecular dynamics simulation to investigate the mechanism of adhesion of three different molecular glues to the MT surface, and the consequent tubulin−tubulin assembly-induced stabilization.

Arg9, **Den9**, and **Asn9** molecular glues bear the same surface groups (nine Gu^+ ions) and owe their ability to stick to the MT surface to the same kind of interaction with the tubulin amino acids (salt bridges). However, they differ on the backbone structure and on the shape assumed in solution. In particular, **Den9** and **Asn9** appear as folded globular molecules, while **Arg9** maintains its linear character.

Importantly, our results demonstrate that different shape molecular glues stick differently on the MT surface, controlling the formation of two radically different tubulin-based nanostructures upon temperature decreasing. In fact, MTs can be entirely stabilized at low temperature by using globular-like molecular glues (**Den9** and **Asn9**). On the other hand, the linear **Arg9** can stabilize only the single PF, but not the adhesion between different PFs at low temperature. Thus, at 15 °C MTs depolymerize into **Arg9**-stabilized unbound PFs that convolve in solution into stable tubulin rings.

These mechanisms of full MT reinforcement and of MT transformation into a different α/β-tubulin nanostructure upon temperature decreasing are here explained as the result of molecular glue adhesion, and are directly related to the shape assumed by molecular glues in solution. This constitutes an important step to learn how to design *ad hoc* molecular glues for the creation of a variety of protein-based nanomaterials whose structure and properties can be controlled at the single-molecule level (*i.e.*, protein origami).

COMPUTATIONAL METHODS

MD Simulation Protocol and Study of Molecular Glues in Solution. The computational strategy adopted for this complex study is based on the simulation approach reported recently by our group for investigating the adhesion of positively charged dendrons to the negatively charged protein surface of capsid CCMV viruses.[20]

The entire simulation work was conducted using the AMBER 11 software.[38] First, we created and parametrized the molecular models for **Arg9**, **Den9**, and **Asn9** molecular glues (all bearing a positive total charge of +9e at neutral pH) according to a validated procedure for the simulation study of polymeric and dendritic molecules interacting with biological targets.[20,39,40] In particular, **Den9** and **Asn9** molecular glues were parametrized according to the "general AMBER force field (GAFF)" (*gaff.dat*).[41] The *parm99* all-atom force field (*leaprc.ff99*)[42] was used to parametrize the **Arg9** molecular glue and all the other standard residues present in the simulated molecular systems.

TABLE 2. Main Features of the Molecular Systems Simulated in This Work

molecular system	simulation temperature (°C)	total molecular glue charge[a] (e)	tubulin total charge (e)	box volume (Å^3)	number of neutralization (Na^+ or Cl^-) ions in the system[b]	number of water molecules in the system	total number of atoms in the system	simulation time for each MD run (ns)
Den9	37 and 15[c]	+9	0	258750	9 Cl^-	8167	24897	100
Arg9	37 and 15[c]	+9	0	106280	9 Cl^-	3357	10302	500
Asn9	37 and 15[c]	+9	0	131328	9 Cl^-	4100	12726	100
MT	37 and 15[c]	0	−152	1679444	152 Na^+	39393	171934	100
MT+Den9	37 and 15[d]	+18	−152	1800346	134 Na^+	43126	183883	100
MT+Arg9	37 and 15[d]	+18	−152	1802303	134 Na^+	43301	184078	100
MT+Asn9	37 and 15[d]	+18	−152	1793710	134 Na^+	42930	183301	100
Tub1&Tub2+Arg9[e]	37 and 15	+9	−76	913740	65 Na^+	22339	94039	100
PF+Arg9	15[f]	+27	−76	1521794	49 Na^+	42675	155534	200

[a] At pH = 7.4 (neutral) each glue molecule is assumed to carry a total +9e positive charge. The total molecular glue charge is given by the sum of the positive charges present over all the glue molecules present in the system. [b] The minimum amount of counterions is added to the systems to guarantee system neutrality. [c] Molecular glues and the MT region used for building the complex systems were preliminarily equilibrated in solution at 37 °C; additional MD simulations were run also at 15 °C for sake of energetic analysis. [d] The MT+molecular glue systems were simulated first at 37 °C for 100 ns and then at 15 °C for other 100 ns. [e] The other seven possible configurations for **Arg9** in binding site **1** were explored by simulating as many reduced size systems composed of **Tub1** and **Tub2** and one **Arg9** molecule. [f] The molecular model for the **Arg9**-reinforced protofilament (PF) was simulated for 200 ns of NPT MD simulation at 15 °C.

The three molecular glue models were immerged in a periodic box containing explicit TIP3P water molecules[43] and 9 Cl^- counterions for neutralization by using the *leap* module of AMBER 11. After preliminary minimization, all systems were initially heated for 50 ps of NVT MD simulation to reach the experimental temperature of 37 °C. During this step the solute was maintained as fixed. All restraints were then removed, and all molecular glues were equilibrated by running NPT MD simulations at the experimental temperature of 37 °C and 1 atm of pressure under periodic boundary conditions. The simulation time of 100 ns was enough to guarantee that **Den9** and **Asn9** molecular glues reached successfully the equilibrium. On the other hand, a longer MD simulation was necessary in the case of **Arg9** (a total of 500 ns were run to guarantee that the equilibrium was reached). The root-mean-square deviation (RMSD) and radius of gyration (R_g) data extracted from the MD trajectories with the *ptraj* module of AMBER 11 were used to verify that each molecule reached the equilibrium with good stability (full RMSD and R_g data are provided in the SI). All equilibration MD runs used a time step of 2 fs, the Langevin thermostat, and a 10 Å cutoff. The particle mesh Ewald[44] (PME) approach was used to treat the long-range electrostatic effects, and the SHAKE algorithm was used on the bonds involving hydrogen atoms.[45] All MD simulations were carried out using the *pmemd.cuda* module working on GTX580 GPU cards. The same simulation protocol was adopted also for all the other MD simulations conducted in this work. All molecular glue solvated systems were simulated also at 15 °C in order to obtain MD trajectories at low temperature useful for the energetic analysis (see next section).

Construction, MD Simulation, and Analysis of the MT-Glue Molecular Systems. Consistent with our previously validated strategy,[20] we obtained an atomistic model for the MT surface. The molecular model of a 13-PFs MT (Figure 2b in the paper) was built as described in detail in previous reports,[26−30,46] *i.e.*, by docking the structure of a α/β-tubulin dimer (PDB code: 1JFF)[47] onto a 13-protofilament electron microscopy EM-map (EM Data Bank code: EMDB-5193)[26] using the UCSF Chimera software.[48]

Since all molecular glues carry an overall positive charge of +9e at neutral pH, negatively charged regions on the MT surface constitute potential binding sites for the glue molecules. In order to study both the intra-PF and inter-PFs reinforcement induced by molecular glue adhesion, a portion of MT was selected for the MD simulations as composed of four α/β-tubulin dimers belonging to two laterally bound PFs (**PF1** and **PF2**, Figure 2b in the main text).[29,30] A periodic box was built around the MT portion composed of **Tub 1**, **Tub 2**, **Tub 3**, and **Tub 4** with 0 Å lateral buffer from the tubulin atoms, and with a 12 Å buffer perpendicular to the MT surface. The periodic box was filled with TIP3P explicit solvent molecules and Na^+ counterions for system neutrality. According to the same simulation protocol described previously, the MT system was preliminarily equilibrated by running a 100 ns NPT MD simulation in periodic boundary conditions, at 37 °C and 1 atm of pressure (an additional simulation was run also at 15 °C in order to obtain one additional MD trajectory for the MT system at low temperature useful for further energetic analysis: see next section).

After we obtained an equilibrated configuration for the MT wall, the solvent was removed from the system. The electrostatic potential in the MT selected region (Figure 2c in the paper) was then calculated using the Adaptive Poisson−Boltzmann Solver (APBS plugin version 1.1)[31] and the PDB2PQR web portal (http://kryptonite.nbcr.net/pdb2pqr/).[49] Considering **Tub1** as reference protein, we identified two binding sites (**1** and **2**, between tubulins **α1** and **α2**, and between **β1** and **α4**, respectively) where the adhesion of molecular glue to the neighbor tubulins might reinforce the protein−protein assembly both along the same PF and between different PFs (Figure 2c).

According to our approach,[20] two equilibrated **Arg9**, **Den9**, and **Asn9** molecules were placed in close vicinity of the MT surface in correspondence of **1** and **2** binding sites (Figure 2 in the paper). This molecular glue-**Tub 1** 2:1 stoichiometry was consistent with the experiments.[23] The obtained molecular systems were again solvated with explicit solvent molecules as described previously (with 0 Å lateral buffer from the tubulin proteins, and with a 12 Å buffer from the molecular glue more distant atom from the MT surface), resulting in three molecular systems (**MT+Den9**, **MT+Arg9** and **MT+Asn9**) containing the MT slice, two glue molecules (**Arg9**, **Den9**, and **Asn9**), and explicit solvent molecules (TIP3P water molecules and neutralizing ions: see Table 2).

After preliminary minimization and heating, all systems were equilibrated for 100 ns of NPT MD simulation at 37 °C and 1 atm of pressure. The simulation protocol was the same described in the previous section for the simulation of molecular glues in water. During the MD runs, all systems successfully reached the equilibrium, and the molecular glues showed strong adhesion to the MT surface. RMSD data and the convergence of the interaction energies (ΔG) extracted from the MD simulations were used to check the systems equilibration (see SI).

Consistent with the experiments, the temperature was then decreased to 15 °C, and each system underwent additional 100 ns of NPT MD simulation. These simulated systems provided useful information on the adhesion of **Arg9**, **Den9**, and **Asn9** to the MT surface, and on the tubulin−tubulin reinforcement induced at low temperature.

As explained in the text, seven other starting configurations/poses were tested for **Arg9** in correspondence of binding site **1** by running as many independent MD simulations (see SI, Figure S6). These seven additional MD simulations accounted for reduced **MT**+**Arg9** molecular systems considering only binding site **1**, the critical one for PF−PF assembly reinforcement according to our scheme. These reduced simulated systems (**Tub1&Tub2**+**Arg9**) consist of **Tub 1** and **Tub 2**, and of a single **Arg9** molecule. Each **Tub1&Tub2**+**Arg9** system was solvated and simulated according to the same protocol used for the other cases.

One additional molecular system was also created to study the behavior of a single PF reinforced with **Arg9** molecular glue in solution. In this case, **PF2** (**Tub 2** and **Tub 3**) was deleted from the system equilibrated at 15 °C. Only **Tub1** and **Tub4**, belonging to **PF1**, were thus considered. One additional **Arg9** molecule (**Arg9$_3$**) was added along the PF for symmetry (Figure 5b in the main paper). The resulting **Arg9**-bound **PF1** was immerged into a periodic water box extending 15 Å in all three directions from the solute atoms. This system was equilibrated for 200 ns of NPT MD simulation at 15 °C and 1 atm of pressure in order to allow for the study of eventual PF deformations. The **Arg9**-reinforced PF bending angle (φ) was calculated as previously reported in the literature.[46] The reported φ average value for the inter-α/β-tubulin-dimer angle was calculated from the equilibrated phase MD simulation (*i.e.*, the last 100 ns) by using the *ptraj* module of AMBER 11 (see SI). Table 2 reports the main features of all simulated systems.

All binding energies (ΔG) were extracted directly from the MD simulations according to a well-validated procedure for the calculation of the interactions between polymeric and dendritic molecules with biological targets.[29,39,40] In particular, ΔG data were obtained from 250 snapshots taken from the equilibrated phase MD trajectories (the last 50 ns of each simulation run at 37 and 15 °C) according to the MM-PBSA approach.[50] Full ΔG adhesion data and detailed information about the energetic analysis procedure adopted are provided in the SI.

Reported ΔG values for **Arg9** adhesion to the MT surface in binding site **1** are averaged over a total of eight MD simulations related to as many different starting configurations studied for **Arg9** molecular glue in this particular case. Molecular glue-induced reinforcement of tubulin−tubulin assembly along individual PFs, and between different PFs, was evaluated as the energetic adhesion of each glue molecule to the single proteins in the MT structure (ΔG_{nn} in Figure 3). The $\Delta G_{\beta 1}$, $\Delta G_{\alpha 4}$, $\Delta G_{\alpha 1}$ and $\Delta G_{\alpha 2}$ calculated values reported in Table 1 were obtained *via* simple decomposition of the adhesion energies ΔG on a per-tubulin basis.

Conflict of Interest: The authors declare no competing financial interest.

Supporting Information Available: Detailed energetic analysis procedure. Full energy data for molecular glue adhesion to the MT surface (ΔG). Full R_g and RMSD data, and additional snapshots taken from the MD simulations. This material is available free of charge *via* the Internet at http://pubs.acs.org.

Acknowledgment. This work was partially supported by the MEXT Grant-in-Aid for Research Activity Start-up (23850007) to K.O.

REFERENCES AND NOTES

1. Keten, S.; Xu, Z.; Ihle, B.; Buehler, M. J. Nanoconfinement Controls Stiffness, Strength and Mechanical Toughness of Beta-Sheet Crystals in Silk. *Nat. Mater.* **2010**, *9*, 359–367.
2. Gautieri, A.; Vesentini, S.; Redaelli, A.; Buehler, M. J. Hierarchical Structure and Nanomechanics of Collagen Microfibrils from the Atomistic Scale Up. *Nano Lett.* **2011**, *11*, 756–766.
3. Winfree, E.; Liu, F.; Wenzler, L. A.; Seeman, N. C. Design and Self-Assembly of Two-Dimensional DNA Crystals. *Nature* **1998**, *394*, 539–544.
4. Rothemund, P. W. K. Folding DNA to Create Nanoscale Shapes and Patterns. *Nature* **2006**, *440*, 297–302.
5. Andersen, E. S.; Dong, M.; Nielsen, M. M.; Jahn, K.; Subramani, R.; Mamdouh, W.; Golas, M. M.; Sander, B.; Stark, H.; Oliveira, C. L. P.; *et al.* Self-Assembly of a Nanoscale DNA Box with a Controllable Lid. *Nature* **2009**, *459*, 73–76.
6. Douglas, S. M.; Dietz, H.; Liedl, T.; Högberg, B.; Graf, F.; Shih, W. M. Self-Assembly of DNA into Nanoscale Three-Dimensional Shapes. *Nature* **2009**, *459*, 414–418.
7. Han, D.; Pal, S.; Nangreave, J.; Deng, Z.; Liu, Y.; Yan, H. DNA Origami with Complex Curvatures in Three-Dimensional Space. *Science* **2011**, *332*, 342–346.
8. Amos, L. A.; Klug, A. Arrangement of Subunits in Flagellar Microtubules. *J. Cell Sci.* **1974**, *14*, 523–549.
9. Hanson, J.; Lowy, J. Structure of F-Actin and of Actin Filaments Isolated from Muscle. *J. Mol. Biol.* **1963**, *6*, 46–60.
10. Chalcroft, J. P.; Engelhardt, H.; Baumeister, W. Structure of the Porin from a Bacterial Stalk. *FEBS Lett.* **1987**, *211*, 53–58.
11. Namba, K.; Stubbs, G. Structure of Tobacco Mosaic-Virus at 3.6-A Resolution: Implications for Assembly. *Science* **1986**, *231*, 1401–1406.
12. Lin, T.; Chen, Z.; Usha, R.; Stauffacher, C. V.; Dai, J.-B.; Schmidt, T.; Johnson, J. E. The Refined Crystal Structure of Cowpea Mosaic Virus at 2.8 Angstrom Resolution. *Virology* **1999**, *265*, 20–34.
13. Dotan, N.; Arad, D.; Frolow, F.; Freeman, A. Self-Assembly of a Tetrahedral Lectin into Predesigned Diamondlike Protein Crystals. *Angew. Chem., Int. Ed.* **1999**, *38*, 2363–2366.
14. Padilla, J. E.; Colovos, C.; Yeates, T. O. Nanohedra: Using Symmetry to Design Self Assembling Protein Cages, Layers, Crystals, and Filaments. *Proc. Natl. Acad. Sci. U. S. A.* **2001**, *98*, 2217–2221.
15. Ringler, P.; Schulz, G. E. Self-Assembly of Proteins into Designed Networks. *Science* **2003**, *302*, 106–109.
16. Uchida, N.; Okuro, K.; Niitani, Y.; Ling, X.; Ariga, T.; Tomishige, M.; Aida, T. Photoclickable Dendritic Molecular Glue: Noncovalent-to-Covalent Photochemical Transformation of Protein Hybrids. *J. Am. Chem. Soc.* **2013**, *135*, 4684–4687.
17. Suzuki, Y.; Okuro, K.; Takeuchi, T.; Aida, T. Friction-Mediated Dynamic Disordering of Phospholipid Membrane by Mechanical Motions of Photoresponsive Molecular Glue: Activation of Ion Permeation. *J. Am. Chem. Soc.* **2012**, *134*, 15273–15276.
18. Okuro, K.; Kinbara, K.; Takeda, K.; Inoue, Y.; Ishijima, A.; Aida, T. Adhesion Effects of a Guanidinium Ion Appended Dendritic "Molecular Glue" on the ATP-Driven Sliding Motion of Actomyosin. *Angew. Chem., Int. Ed.* **2010**, *49*, 3030–3033.
19. Kostiainen, M. A.; Kasyutich, O.; Cornelissen, J. J.; Nolte, R. J. Self-Assembly and Optically Triggered Disassembly of Hierarchical Dendron-Virus Complexes. *Nat. Chem.* **2010**, *2*, 394–399.
20. Doni, G.; Kostiainen, M. A.; Danani, A.; Pavan, G. M. Generation-Dependent Molecular Recognition Controls Self-Assembly in Supramolecular Dendron-Virus Complexes. *Nano Lett.* **2011**, *11*, 723–728.
21. Kirschne, M. W.; Williams, R. C.; Weingart, M.; Gerhert, J. C. Microtubules from Mammalian Brain: Some Properties of Their Depolymerization Products and a Proposed Mechanism of Assembly and Disassembly. *Proc. Natl. Acad. Sci. U. S. A.* **1974**, *71*, 1159–1163.
22. Okuro, K.; Kinbara, K.; Tsumoto, K.; Ishii, N.; Aida, T. Molecular Glues Carrying Multiple Guanidinium Ion Pendants *via* an Oligoether Spacer: Stabilization of Microtubules against Depolymerization. *J. Am. Chem. Soc.* **2009**, *131*, 1626–1627.
23. Ishii, N.; Okuro, K.; Kinbara, K.; Aida, T. Image Analysis of Alpha/Beta-Tubulin Rings in Two-Dimensional Crystalline Arrays of Periodic Mesoporous Nanostructures. *J. Biochem.* **2010**, *147*, 555–563.
24. Garzoni, M.; Cheval, N.; Fahmi, A.; Danani, A.; Pavan, G. M. Ion-Selective Controlled Assembly of Dendrimer-Based Functional Nanofibers and Their Ionic-Competitive Disassembly. *J. Am. Chem. Soc.* **2012**, *134*, 3349–3357.
25. Pavan, G. M.; Barducci, A.; Albertazzi, L.; Parrinello, M. Combining Metadynamics Simulation and Experiments

to Characterize Dendrimers in Solution. *Soft Matter* **2013**, *9*, 2593–2597.
26. Sui, H.; Downing, K. H. Structural Basis of Interprotofilament Interaction and Lateral Deformation of Microtubules. *Structure* **2010**, *18*, 1022–1031.
27. Wells, D. B.; Aksimentiev, A. Mechanical Properties of a Complete Microtubule Revealed through Molecular Dynamics Simulation. *Biophys. J.* **2010**, *99*, 629–637.
28. Chacón, P.; Wriggers, W. Multi-Resolution Contour-Based Fitting of Macromolecular Structures. *J. Mol. Biol.* **2002**, *317*, 375–384.
29. Magnani, M.; Maccari, G.; Andreu, J. M.; Diaz, J. F.; Botta, M. Possible Binding Site for Paclitaxel at Microtubule Pores. *FEBS J.* **2009**, *276*, 2701–2712.
30. Maccari, G.; Mori, M.; Rodriguez-Salarichs, J.; Fang, W. S.; Diaz, J. F.; Botta, M. Free Energy Profile and Kinetics Studies of Paclitaxel Internalization from the Outer to the Inner Wall of Microtubules. *J. Chem. Theory Comput.* **2013**, *9*, 698–706.
31. Baker, N. A.; Sept, D.; Joseph, S.; Holst, M. J.; McCammon, J. A. Electrostatics of Nanosystems: Application to Microtubules and the Ribosome. *Proc. Natl. Acad. Sci. U. S. A.* **2001**, *98*, 10037–10041.
32. Tomalia, D. A. In Quest of a Systematic Framework for Unifying and Defining Nanoscience. *J. Nanopart. Res.* **2009**, *11*, 1251–310.
33. Tomalia, D. A. Dendritic Effects: Dependency of Dendritic Nano-Periodic Property Patterns on Critical Nanoscale Design Parameters (CNDPs). *New J. Chem.* **2012**, *36*, 264–281.
34. Nicholson, W. V.; Lee, M.; Downing, K. H.; Nogales, E. Cryo-Electron Microscopy of GDP-Tubulin Rings. *Cell Biochem. Biophys.* **1999**, *31*, 175–183.
35. Nogales, E.; Wang, H.-W.; Niederstrasser, H. Tubulin Rings: Which Way Do They Curve? *Curr. Opin. Struct. Biol.* **2003**, *13*, 256–261.
36. Erickson, H. P.; Stoffler, D. Protofilaments and Rings, Two Conformations of the Tubulin Family Conserved from Bacterial FtsZ to Alpha/Beta and Gamma Tubulin. *J. Cell Biol.* **1996**, *135*, 5–8.
37. Gigant, B.; Curmi, P. A.; Martin-Barbey, C.; Charbaut, E.; Lachkar, S.; Lebeau, L.; Siavoshian, S.; Sobel, A.; Knossow, M. The 4 Angstrom X-Ray Structure of a Tubulin: Stathmin-like Domain Complex. *Cell* **2000**, *102*, 809–816.
38. Case, D. A.; Darden, T. A.; Cheatham, T. E., III; Simmerling, C. L.; Wang, J.; Duke, R. E.; Luo, R.; Walker, R. C.; Zhang, W.; Merz, K. M.; *et al. AMBER 11*; University of California: San Francisco, 2010.
39. Zheng, M.; Pavan, G. M.; Neeb, N.; Schaper, A. K.; Danani, A.; Klebe, G.; Merkel, O. M.; Kissel, T. Targeting the Blind Spot of Polycationic Nanocarrier-Based siRNA Delivery. *ACS Nano* **2012**, *6*, 9447–9454.
40. Kostiainen, M. A.; Kotimaa, J.; Laukkanen, M. L.; Pavan, G. M. Optically Degradable Dendrons for Temporary Adhesion of Proteins to DNA. *Chem.—Eur. J.* **2010**, *16*, 6912–6918.
41. Wang, J.; Wolf, R. M.; Caldwell, J. W.; Kollman, P. A.; Case, D. A. Development and Testing of a General Amber Force Field. *J. Comput. Chem.* **2004**, *25*, 1157–1174.
42. Cheatham, T. E.; Cieplak, P.; Kollman, P. A. A Modified Version of the Cornell *et al.* Force Field with Improved Sugar Pucker Phases and Helical Repeat. *J. Biomol. Struct. Dyn.* **1999**, *16*, 845–862.
43. Jorgensen, W. L.; Chandrasekhar, J.; Madura, J. D.; Impey, R. W.; Klein, M. L. Comparison of Simple Potential Functions for Simulating Liquid Water. *J. Chem. Phys.* **1983**, *79*, 926–935.
44. Darden, T.; York, D.; Pedersen, L. Particle Mesh Ewald: An *N* log(*N*) Method for Ewald Sums in Large Systems. *J. Chem. Phys.* **1993**, *98*, 10089–10092.
45. Krautler, V.; van Gunsteren, W. F.; Hunenberger, P. H. A Fast SHAKE Algorithm to Solve Distance Constraint Equations for Small Molecules in Molecular Dynamics Simulations. *J. Comput. Chem.* **2001**, *22*, 501–508.
46. Grafmüller, A.; Voth, G. A. Intrinsic Bending of Microtubule Protofilaments. *Structure* **2011**, *19*, 409–417.
47. Lowe, J.; Li, H.; Downing, K. H.; Nogales, E. Refined Structure of Alpha Beta-Tubulin at 3.5 A Resolution. *J. Mol. Biol.* **2001**, *313*, 1045–1057.
48. Pettersen, E. F.; Goddard, T. D.; Huang, C. C.; Couch, G. S.; Greenblatt, D. M.; Meng, E. C.; Ferrin, T. E. UCSF Chimera—A Visualization System for Exploratory Research and Analysis. *J. Comput. Chem.* **2004**, *25*, 1605–1612.
49. Dolinsky, T. J.; Nielsen, J. E.; McCammon, J. A.; Baker, N. A. PDB2PQR: An Automated Pipeline for the Setup of Poisson-Boltzmann Electrostatics Calculations. *Nucleic Acids Res.* **2004**, *32*, W665–W667.
50. Kollman, P. A.; Massova, I.; Reyes, C.; Kuhn, B.; Huo, S. H.; Chong, L.; Lee, M.; Lee, T.; Duan, Y.; Wang, W.; *et al.* Calculating Structures and Free Energies of Complex Molecules: Combining Molecular Mechanics and Continuum Models. *Acc. Chem. Res.* **2000**, *33*, 889–897.
51. Tomalia, D. A.; Naylor, A. M.; Goddard, W. A. Starbust Dendrimers: Molecular-Level Control of Size, Shape, Surface-Chemistry, Topology, and Flexibility from Atoms to Macroscopic Matter. *Angew. Chem., Int. Ed.* **1990**, *29*, 138–175.
52. Buhleier, E.; Wehner, W.; Vögtle, F. "Cascade"- and "Nonskid-Chain-like" Syntheses of Molecular Cavity Topologies. *Synthesis* **1978**, *2*, 155–158.
53. Lim, J.; Pavan, G. M.; Annunziata, O.; Simanek, E. E. Experimental and Computational Evidence for an Inversion in Guest Capacity in High Generation Triazine Dendrimer Hosts. *J. Am. Chem. Soc.* **2012**, *134*, 1942–1945.